Continuous-wave diode-pumped Yb:$LuVO_4$ lasers

Junhai Liu,[a)] Valentin Petrov,[a)] Xavier Mateos,[a)] Huaijin Zhang,[b)] Jiyang Wang,[b)]
Minhua Jiang,[b)] Sabine Miller,[a)] Guibao Xu,[a)] Uwe Griebner,[a)] Frank Noack[a)]

[a]Max-Born-Institute for Nonlinear Optics and Ultrafast Spectroscopy,
2A Max-Born-Str., D-12489 Berlin, Germany;
[b]National Laboratory of Crystal Materials, Shandong University, Jinan 250100, China

ABSTRACT

We studied several crystals of Yb-doped $LuVO_4$ with different orientations (*a*-cut and *c*-cut) in order to evaluate the potential of this new laser material for high power continuous-wave operation using simple hemispherical cavities, longitudinally pumped by a fiber coupled diode laser. We achieved substantial improvement with respect to previous results in terms of output power and slope efficiency. The highest output power and optical efficiency were obtained for the π-polarization using *a*-cut samples. Bistability of the input-output power characteristics in terms of a hysteresis loop was also observed. Significant intensity fluctuations were found existing in a small operational region near the critical point (up-threshold) of the bistability region. The heating of the crystal is reduced in the lasing state when stimulated emission keeps the part of the radiative relaxation high in comparison to the nonradiative relaxation processes.

Key words: Yb-lasers; diode-pumped lasers; $LuVO_4$; optical bistability.

1. INTRODUCTION

The crystal of $LuVO_4$ is a member of the orthovanadate family of zircon ($ZrSiO_4$) tetragonal structure $I4_1/amd$ (point group 4/*mmm*). It was first developed as a laser host material for the trivalent neodymium ion (Nd^{3+}) in 2002.[1] Spectroscopic studies of Nd:$LuVO_4$ indicated larger absorption cross section near 800 nm and larger emission cross section at 1.064 µm in comparison with both Nd:YVO_4 and Nd:$GdVO_4$.[1] These features are very desirable for diode-pumped solid-state lasers, as they make it feasible to achieve highly efficient pumping and to realize low threshold laser operation with high optical-to-optical efficiency. High-power efficient laser operation of Nd:$LuVO_4$ has been realized with diode-pumping in the continuous-wave (cw) as well as in the pulsed (Q-switched) operational regimes.[2] In 2006, $LuVO_4$ was doped also with thulium (Tm^{3+}) and with diode-pumping in the same 800 nm spectral range, cw laser operation near 1.9 µm was achieved.[3]

Very recently, all the three vanadate crystals (YVO_4, $GdVO_4$, and $LuVO_4$) were demonstrated to be promising laser host materials for the ytterbium ion (Yb^{3+}).[4–7] The major advantages of Yb-doped vanadates, compared to Yb:YAG which has been widely employed since the early days of Yb-lasers, are the higher absorption and emission cross sections and the broader bandwidths, the small quantum defect which results from the much closer wavelengths of excitation and emission, and the inherent polarized oscillation arising from the strong anisotropy in the emission spectra. Additionally, Yb-doped vanadates are also advantageous in thermal load management when compared to Yb-doped monoclinic potassium double tungstates [$KY(WO_4)_2$, $KGd(WO_4)_2$, $KLu(WO_4)_2$] owing to their 1.5–2.5 times higher thermal conductivities and their lower thermo-mechanical anisotropy.

From the point of view of crystal growth, Yb:$LuVO_4$ is the most promising among the Yb-doped vanadates. The closeness of the Lu and Yb ions in ionic radius and mass is likely to lead to not only less lattice distortion, but also less reduction in thermal conductivity by the ion substitution. The effect of thermal conductivity reduction by Yb doping has

Solid State Lasers XVI: Technology and Devices, edited by Hanna J. Hoffman, Ramesh K. Shori, Norman Hodgson,
Proc. of SPIE Vol. 6451, 64511B, (2007) · 0277-786X/07/$15 · doi: 10.1117/12.700048

been known to be considerable for Yb:YAG, a moderate doping level of 3 at. % will reduce the thermal conductivity to 60% of that for the undoped crystal.[8]

We present in this paper the results on highly efficient cw laser operation achieved with both *a*-cut and *c*-cut Yb:$LuVO_4$ crystals at room temperature under end-pumping by a high-power diode laser. Polarized laser radiation was generated with *c*-cut crystals despite the nominal optical isotropy in the plane perpendicular to the *c*-axis. Optical bistability was encountered in the laser operation of Yb:$LuVO_4$, which has been found later existing also in lasers realized with the other Yb-doped vanadates.

2. OPTICAL AND SPECTROSCOPIC PROPERTIES

Yb:$LuVO_4$ crystals were grown by the conventional Czochralski method. The starting polycrystalline charges of $LuVO_4$ and $YbVO_4$, synthesized from high purity (99.99%) Lu_2O_3, Yb_2O_3, and V_2O_5 compounds through the liquid-phase method, were mixed according to the chemical formula $Yb_{0.015}Lu_{0.985}VO_4$. Both *a*- and *c*-axis grown Yb:$LuVO_4$ crystals of high optical quality were obtained with boule sizes of about ϕ 20×20 mm. The actual Yb concentration in the crystals was measured to be 1.56 at. %, corresponding to an ion density of 2.04×10^{20} cm^{-3}.

Transmission measurements of undoped $LuVO_4$ can be found in the corresponding literature.[9] $LuVO_4$ is transparent from about 0.35 to 15 µm. The ordinary and extraordinary refractive indices are 2.031 and 2.249, respectively.[9] We estimated the Kerr type nonlinearity n_2 of Yb:$LuVO_4$ using the *Z*-scan technique in the thin sample approximation, see Fig. 1.[10] The pulses at 1064 nm from an active-passive mode-locked Nd:YAG laser operating at 10 Hz had a duration of 15 ps. 1- and 2-mm thick samples of *a*-cut Yb:$LuVO_4$ were used which allowed to measure two components of this tensor, for propagation along the *a*-axis. The results for the two thicknesses were very close. Averaging over 5 independent measurements for each of the possible polarization orientations we obtained: $n_2(E//c)=1.08\times10^{-15}$ cm^2/W and $n_2(E\perp c)=1.34\times10^{-15}$ cm^2/W with deviations of ±10%. These values are roughly 30% lower than the corresponding results reported for 2 at. % Yb-doped YVO_4,[11] but almost in the same proportion.

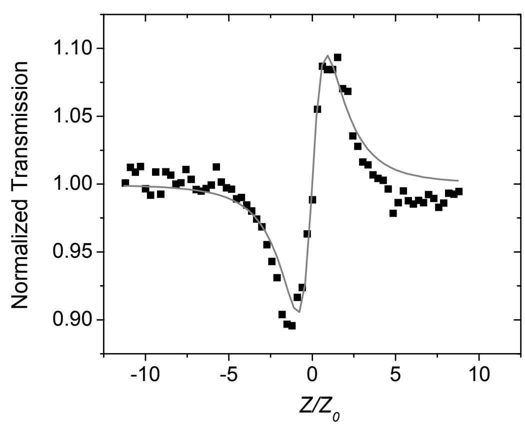

Fig. 1. Measured Z-scan for the 2-mm thick Yb:$LuVO_4$ sample and $E\perp c$ (Z_0 denotes the Rayleigh length).

In Yb-doped laser media, the absorption spectrum usually overlaps significantly with the emission spectrum. This property leads to re-absorption resulting in radiation trapping. To measure the fluorescence lifetime of such laser media, special precautions must be taken to eliminate the lengthening effect caused by radiation trapping. We measured the fluorescence lifetime of Yb:$LuVO_4$ by use of the "pinhole technique",[4] giving a result of τ = 256 ±11 µs, which is very close to that measured for Yb:YVO_4 by using crystal powders.[5]

For spectroscopic measurement, *a*-cut crystal samples of 1.5 and 6 mm thickness were prepared from the *a*-grown Yb:$LuVO_4$ boule. The room-temperature polarized absorption spectra of Yb:$LuVO_4$ were measured employing a Lambda 900 UV/VIS/NIR spectrometer. The absorption cross sections, calculated from the measured spectra and the

Yb-concentration, are presented in Fig. 2. The spectra exhibit pronounced anisotropy; the absorption is much stronger for the π-polarization ($E//c$) than for the σ-polarization ($E \perp c$). The main absorption band for the π-polarization is centered at 985 nm with a peak cross section of 8.42×10^{-20} cm^2 and a FWHM of 7.3 nm. For σ-polarization, the main absorption band is much wider; its peak locates at 969 nm with a cross section of 1.97×10^{-20} cm^2, while the narrower 985-nm band has a peak cross section of 2.08×10^{-20} cm^2. Figure 2 also presents the polarized stimulated emission cross sections, computed by use of the modified reciprocity method.[5] The peak emission cross section for both σ- and π-polarizations is at 985 nm, with $\sigma_{em}(\pi) = 11.8\times10^{-20}$ cm^2 and $\sigma_{em}(\sigma) = 3.5\times10^{-20}$ cm^2. In the emission wavelength range of 1020-1055 nm which is of interest for laser oscillation, $\sigma_{em}(\pi) = 10.3\ldots2.0\times10^{-21}$ cm^2.

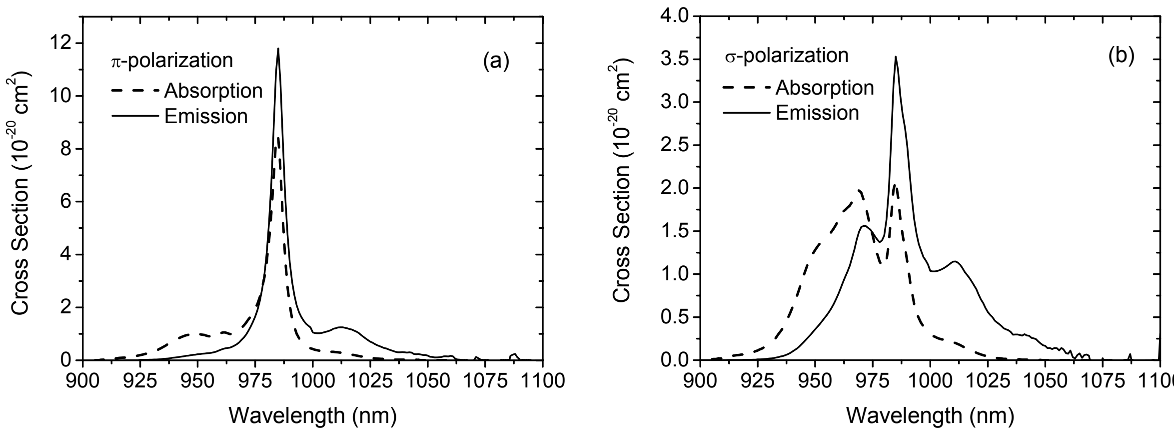

Fig. 2. Polarized absorption and emission cross sections of $Yb:LuVO_4$ measured at room temperature: (a) π and (b) σ.

3. EXPERIMENTAL SETUP

A plano-concave resonator was employed in the experiment to study the laser performance of $Yb:LuVO_4$ crystals. Figure 3 illustrates the experimental arrangement. The plane mirror had a dielectric coating highly reflecting for 1015-1230 nm (> 99.8%) and highly transmitting for 880-990 nm (> 97%). As the output coupler, several concave mirrors of radius-of-curvature of 50 mm with transmission of 0.5%─10% at 1030 nm were used. The cavity length was about 50 mm.

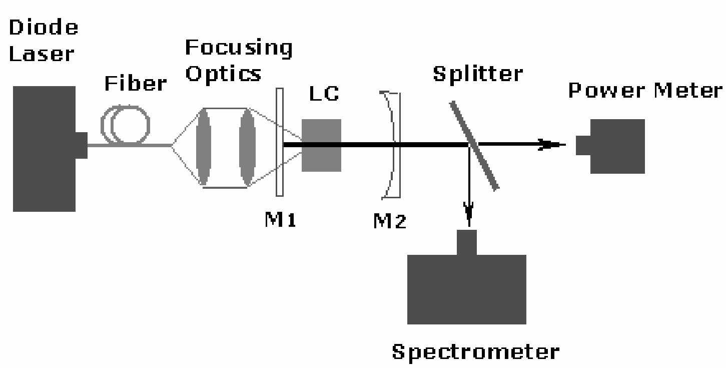

Fig. 3. Schematic diagram of the experimental setup. LC: laser crystal, M1, M2: mirrors.

Both *a*-cut and *c*-cut crystal samples with aperture of 3.3 × 3.3 mm^2 and thickness of 2 mm were prepared from the *c*-axis grown $Yb:LuVO_4$ boule. The uncoated $Yb:LuVO_4$ samples were fixed into a copper holder that was water cooled.

The cooling water was maintained at a temperature of 12°C. The pump source used was a 50-W high-brightness fiber-coupled diode (S50-980-2, Apollo Instruments, Inc., fiber core diameter of 200 μm and NA of 0.22) emitting infrared radiation at 974─981 nm depending on the output level. The pump beam was focused by a 1:1 re-imaging unit and delivered onto the laser crystal which was positioned close to the plane mirror.

4. HIGH-POWER CW LASER PERFORMANCE

We first studied the laser performance of the 2 mm thick *a*-cut Yb:$LuVO_4$ crystal. Figure 4a shows the dependence of the output power (P_{out}) on the absorbed pump power (P_{abs}), measured with decreasing pump power for three output couplings, $T = 2\%$, 5%, and 10%.

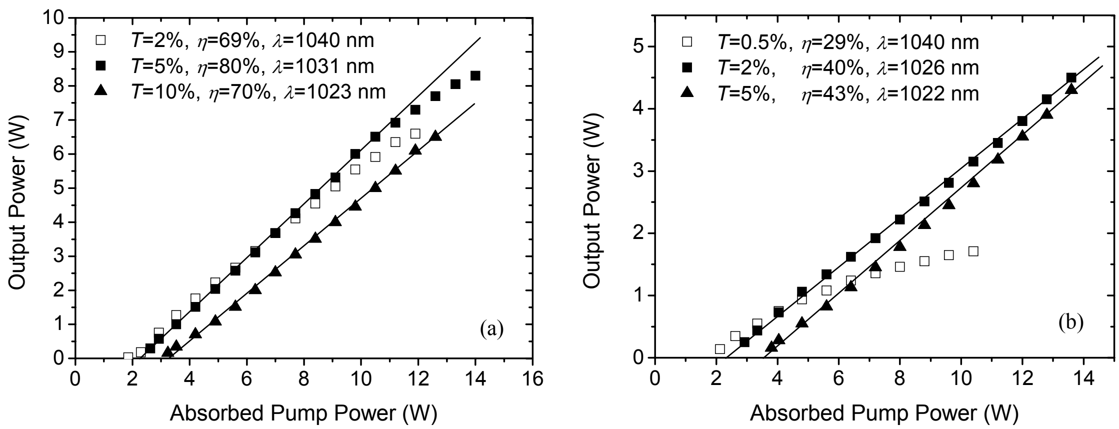

Fig. 4. Output power versus absorbed pump power for the 2-mm thick *a*-cut (a) and *c*-cut (b) Yb:$LuVO_4$ crystals.

The absorbed pump power required for reaching threshold was 1.9, 2.6, and 3.2 W for $T = 2\%$, 5%, and 10%, respectively. For $P_{abs} < 6$ W, the most efficient operation was attained with output coupling of $T = 2\%$; exceeding this level, however, the optimal coupling changed to $T = 5\%$, a slope efficiency as high as 80% was reached for $P_{abs} < 11$ W. When P_{abs} was further increased, the laser became less efficient; the slope efficiency dropped to ~ 50%. This is due to the insufficient cooling of the laser crystal that led to increased reabsorption losses arising from the more populated terminal laser level. Before the output power started to decrease, however, a maximum of 8.3 W was reached at 1031 nm for $P_{abs} = 14$ W, resulting in an optical-to-optical efficiency of 59%. The slope efficiency η in the cases of $T = 2\%$ and 10% was determined to be 69% and 70%. The highest attainable output power for these two cases was also lower than that for $T = 5\%$. The generated laser beam was always linearly polarized along the *c*-axis (π-polarized), independent of the power level and the output coupling used, which is in accordance with earlier results obtained with an *a*-cut Yb:$LuVO_4$ crystal.[7]

Figure 4b shows the output power versus the absorbed pump power obtained with the 2 mm *c*-cut Yb:$LuVO_4$ crystal. The thresholds for $T = 0.5\%$, 2%, and 5%, measured by decreasing the pump power, were 2.1, 2.9, and 3.8 W. The higher thresholds in comparison with the *a*-cut crystal originated from the smaller σ_{em}. From Fig. 4b one can see that the output power was subject to an early saturation in the case of $T = 0.5\%$. The optimal operation was achieved with output coupling of $T = 2\%$, yielding a maximum output power of 4.5 W at $P_{abs} = 13.6$ W, leading to an optical-to-optical efficiency of 33%, the slope efficiency was $\eta = 40\%$. The emission wavelength at this power level was 1026 nm. With a still larger output coupling of $T = 5\%$, the laser operation was slightly more efficient, giving a slope efficiency of 43%, but the highest output power reached was 4.3 W, slightly lower than the one obtained in the case of $T = 2\%$. The emission wavelength shifted to a shorter value of 1022 nm.

Yb:$LuVO_4$ is a uniaxial crystal belonging to the point group 4/mmm. Its optic axis, the *c* axis, is a unique four-fold symmetry axis. As a result, the *a* and *b* axes are indistinguishable; accordingly, the plane determined by *a* and *b* is optically isotropic. Considering these facts, one might expect an unpolarized output beam to be generated with the *c*-cut crystal. However, this is not the case. Instead of being unpolarized, the laser radiation was actually linearly polarized along [110] direction; under sufficiently strong pumping, the second polarization component parallel to $[\bar{1}10]$ direction would start oscillating, and the laser entered a region in which the two orthogonal polarization components oscillated simultaneously.

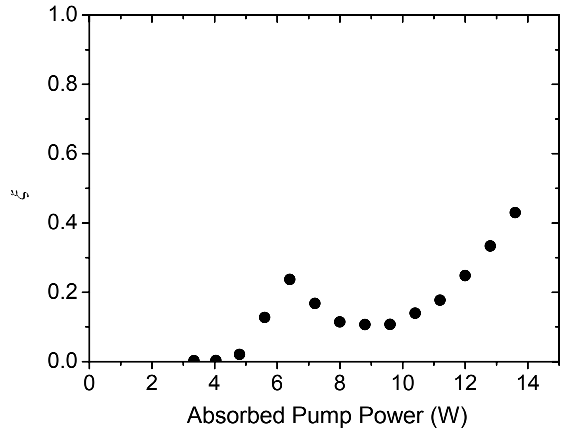

Fig. 5. Variation of the output power ratio (ξ) between the two orthogonal polarizations along $[\bar{1}10]$ and [110] directions with absorbed pump power. The output coupler had $T = 2\%$.

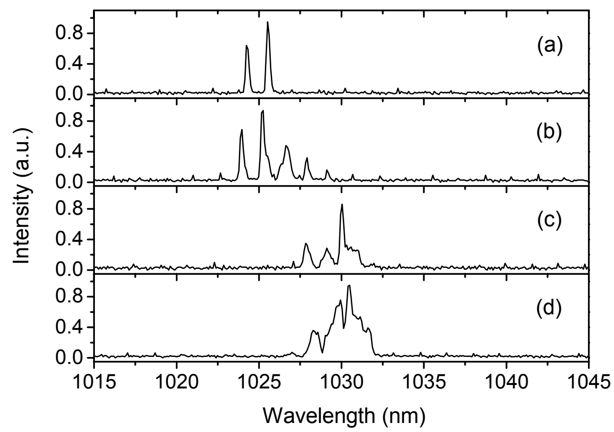

Fig. 6. Laser emission spectra of the two orthogonal polarization components recorded with output coupling $T = 2\%$: (a) $[\bar{1}10]$, $P_{abs} = 4.8$ W, $P_{out} = 0.02$ W; (b) [110], $P_{abs} = 4.8$ W, $P_{out} = 1.04$ W; (c) $[\bar{1}10]$, $P_{abs} = 7.2$ W, $P_{out} = 0.28$ W; (d) [110], $P_{abs} = 7.2$ W, $P_{out} = 1.64$ W.

Figure 5 illustrates the variation of the output power ratio between the two polarizations, $\xi = P_{[\bar{1}10]}/P_{[110]}$, measured in the case of $T = 2\%$. Under relatively weak pumping ($P_{abs} < 4.8$ W), ξ remained zero, the laser oscillation was linearly polarized along [110] direction, with a maximum output power up to ~ 1 W. In the high pump power range, $P_{abs} > 4.8$ W, the variation of ξ was not monotonic with the absorbed pump power, it exhibited some sort of oscillating feature. With increasing pump power, ξ increased first to a maximum of ~ 0.24, then dropped gradually to a minimum of ~ 0.11; after that, it increased again, reaching a value of 0.43 at the highest absorbed pump power of 13.6 W, the output powers for polarization along [110] and $[\bar{1}10]$ directions being 3.15 and 1.35 W, respectively.

It was found that the laser emission spectra were distinct for the two orthogonal polarizations. Figure 6 gives the emission spectra recorded at two different pump powers, the output coupling used was $T = 2\%$. For $P_{abs} = 4.8$ W, at which the $[\bar{1}10]$ polarization component just started oscillating with an output power of 0.02 W, its emission spectrum consisted of two lines centered at 1024.3 and 1025.5 nm whereas for the [110] polarization the spectrum was made up of five discrete lines located at 1023.9, 1025.2, 1026.6, 1027.9, and 1029.1 nm. For an intermediate pumping level of $P_{abs} = 7.2$ W, the individual emission lines became overlapped, with the peak wavelength shifted to 1030 and 1030.5 nm for $[\bar{1}10]$ and [110] polarization components, respectively.

The linearly polarized laser oscillation obtained with the *c*-cut Yb:$LuVO_4$ crystal is attributed to the existence of some degree of birefringence in the crystal. Similar situations have been encountered in some Nd:YAG microchip lasers, in which the stress induced birefringence in the optically isotropic crystal led to linearly polarized oscillation.[12,13] However, the *c*-cut Yb:$LuVO_4$ laser differs significantly from those Nd:YAG lasers: The polarization directions in the Nd:YAG lasers were determined by the stress exerted on the crystal whereas the lasing polarizations remained parallel to [110] and $[\bar{1}10]$ directions in the case of the *c*-cut Yb:$LuVO_4$, regardless of the direction alteration of the stress exerted through the copper holder. Therefore, the birefringence present in the *c*-cut Yb:$LuVO_4$ crystal might be induced through the elasto-optic effect, by the residual strain formed during crystal growth and/or the processing of the sample.

Placing the crystal between two orthogonal polarizers and using a He-Ne laser as a probe beam, we examined the anisotropy of the *c*-cut Yb:$LuVO_4$ crystal under conditions of no pumping. Just as expected, the crystal did exhibit weak birefringence, with the induced principal axes parallel to the [110] and [$\bar{1}10$] directions, which represent the two orthogonal eigenpolarization directions. This means the $Yb:LuVO_4$ has become, in some sense, a biaxial crystal due to the residual strain. As in a real biaxial laser crystal, the laser oscillates with polarization parallel to these two directions. Because of the similar gain cross sections for the two polarizations, strong polarization competition can be expected in the resultant laser operation: This was evident in our experiment from the substantial variation of the output power ratio between the two polarization components.

From a practical point of view, the *a*-cut $Yb:LuVO_4$ crystal is more advantageous, not only because of the more efficient laser operation with higher attainable output power, but also because of its simple linear polarization nature. On the other hand, however, the *c*-cut $Yb:LuVO_4$ laser oscillating simultaneously in two orthogonal polarizations, may also find some practical applications.

5. OPTICAL BISTABILITY IN LASER OPERATION

We have observed optical bistability in the laser oscillation of $Yb:LuVO_4$ crystals. Similar phenomenon has been found in other types of lasers such as CO_2 lasers, Er-doped fiber lasers, and semiconductor lasers,[14-16] but it has not been encountered, to our knowledge, in solid-state lasers. Usually, such bistable behavior originates from the saturable absorber which is contained in the laser resonator. In the case of the $Yb:LuVO_4$ laser, the resonant reabsorption losses take the role of an effective saturable absorber.

We studied the bistable laser operation by employing a similar but more compact plano-concave resonator with an output coupler having a radius of curvature equal to 25 mm (T = 0.5%). The physical cavity length was 22 mm, far from the hemispherical configuration. The 2 mm thick *a*-cut $Yb:LuVO_4$ crystal (aperture of 4 × 4 mm^2) was antireflection coated for high transmission both near 1040 nm and near 985 nm. Other conditions remained the same as shown in Fig. 3.

In this case, a moderate output power of 3.02 W at an emission wavelength of 1049 nm was obtained for an absorbed pump power of 10.23 W, giving an optical-to-optical efficiency of 29.5%; the slope efficiency was determined to be η=38%. The lower output power and efficiencies are due to the non-hemispherical configuration, which is less favorable for achieving efficient laser operation, but helpful to strengthen the bistable behavior. The output beam was π-polarized in the entire operational range. The emission wavelength shifted progressively from 1039 to 1049 nm with increasing pump power as a consequence of the increasing reabsorption losses which depend on the thermal population of the terminal laser level.

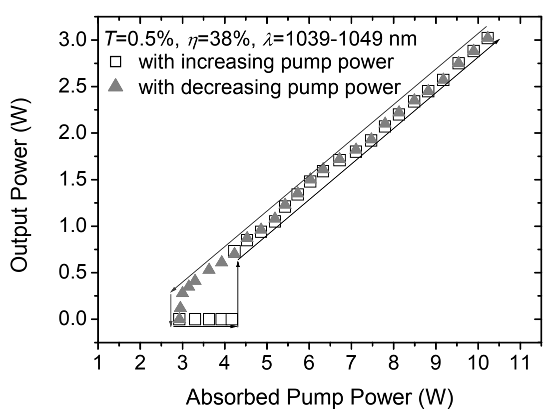

Fig. 7. Dependence of the output power on the absorbed pump power, showing a sizable hysteresis loop.

Figure 7 illustrates the relation between the output power and the absorbed pump power. When the absorbed pump power was increased starting from zero, the laser would not start oscillating until a critical point, referred to as up-threshold, was reached at P_{abs} = $P_{th,up}$ = 4.2 W, at which the output power jumped from zero to a substantial level of 0.73 W. Above this point the output power scaled almost linearly with pump power. If the pump power was reduced starting from a level in excess of $P_{th,up}$, the output power would decrease with nearly the same slope, with the laser still oscillating for pump powers below $P_{th,up}$. Further reduction of the pump power would eventually lead to cessation of the laser oscillation at the down-threshold $P_{th,down}$ = 2.9 W, where the output power dropped from 0.12 W to zero. Therefore, a sizable hysteresis loop in the dependence of the output power on the pump power was present. In the pump power range defined by $P_{th,down} < P_{abs} < P_{th,up}$, the operation of the Yb:$LuVO_4$ laser was bistable; the output power at a given pump level depended on the way this pump level was reached.

For the pump conditions used in the present experiment, a part of the 2-mm thick Yb-doped crystal near its unpumped end would be characterized by much weaker level of inversion and hence increased reabsorption. The inhomogeneous inversion is a consequence of the highly divergent nature of the pump beam and the relatively high crystal absorption. Thus this part of the crystal could play the role of a saturable absorber leading to the bistable operation of the Yb:$LuVO_4$ laser. To verify this explanation, we replaced the 2-mm thick crystal by another one with a thickness of 0.15-mm which was uncoated but had the same doping level, maintaining all the other laser conditions unchanged. In this case, no bistability in the laser operation was observed; the threshold was reached at P_{abs} = 0.9 W with a negligible output, and there was no difference when the pump power was increasing or decreasing. Obviously, as a result of the inversion created along the whole length of the thin crystal, the resonant losses due to reabsorption were greatly reduced in this case. This was confirmed by the substantially shorter oscillation wavelength (λ = 1019 nm) measured with the 0.15-mm thick Yb:$LuVO_4$ crystal. Thus, the observed bistability is related to the presence of (saturable) reabsorption losses in the active medium.

The absorbed pump power required for reaching threshold in the present Yb:$LuVO_4$ laser was quite high, which is expected to cause a significant thermal load inside the crystal. The resulting temperature rise in the crystal might play an important role for the observed optical bistability because the primary effect of changing temperature is the redistribution of the population in the two manifolds leading to increased reabsorption at higher temperature. To investigate the influence of the thermal load, we reduced the average pump power by employing a chopper with a duty cycle of 1/12, rotating at 50 Hz. In this case, the laser reached threshold at much lower pump levels: The absorbed pump powers measured at the up- and down-thresholds, in terms of instantaneous power, were $P_{th,up}$ = 2.21 W and $P_{th,down}$ = 1.65 W. The corresponding instantaneous output power at the up- and down-thresholds was 0.19 and 0 W, respectively. The comparison with the case of true cw operation reveals that the bistability is affected to a great extent by the thermal load which confirms that it is related to the resonant reabsorption losses. It should be noted, however, that although the average absorbed pump power at the up-threshold was only 0.18 W (pump duration ~1.7 ms) and the thermal effect inside the crystal was greatly reduced, it was still possible to observe the hysteresis loop.

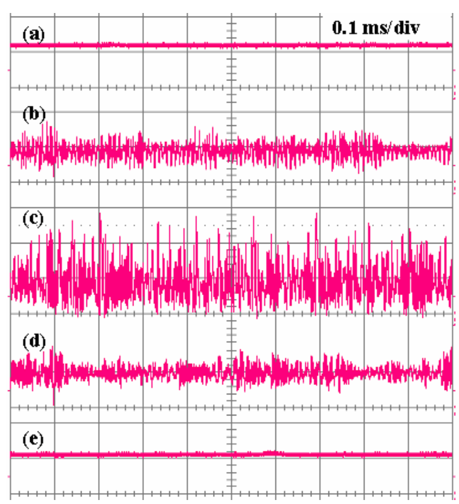

Fig. 8. Oscilloscope traces of the laser output showing the intensity fluctuations near the up-threshold. The traces from (a) to (e) were recorded when the output power was decreased through the up-threshold point. The horizontal time scale is 0.1 ms/div.

The hysteresis loop itself can be qualitatively explained by continuous heating of the crystal followed by stronger reabsorption, which increases the threshold and makes it necessary to further increase the pump level which in turn produces even more heat. In the absence of lasing (below the up-threshold), when increasing the pump power, nonradiative relaxation processes play an important role. In contrast, when starting from the lasing condition and decreasing the pump power, the stimulated emission increases the part of the radiative relaxation suppressing the nonradiative part which leads to less heat production and reduced down-threshold. The real situation is much more complicated because in the threshold regions both the wavelength and the polarization might change during the transition between the two states. The above explanation based on the role of the thermal effects is consistent with the observed narrowing of the hysteresis region to 0.7 and 0.3 W in terms of P_{abs} when the output coupler transmission was increased to T = 1% and 2%, respectively. Nevertheless, the fact that the hysteresis loop was observed also with the chopper means that the physical effect behind the bistability is strongly affected by the temperature but heating is not solely responsible for it.

Bistable operation was clearly predicted within the theoretical model used by Lugiato et al.[17] for a laser having an absorbing medium inside its resonator. Another interesting effect accompanying the bistability are the significant intensity fluctuations expected to occur in the transition region near the critical point (up-threshold).[17] Indeed, such fluctuations were observed in the present Yb:$LuVO_4$ laser on sub-millisecond time scale when passing this region starting from the lasing state. Figure 8 shows a series of oscilloscope traces of the laser output recorded while the pump power was decreased through the up-threshold point [from (a) to (e)]. Near the critical point, the region in which the fluctuations were observed covered a pump power range corresponding to ΔP_{abs} = 0.6 W, the most significant fluctuations occurring close to the up-threshold point.

Table 1. Absorbed pump power at threshold for different Yb-doped crystals (for vanadates, $P_{th} \equiv P_{th,\,up}$)*

Host	$LuVO_4$	$GdVO_4$	YVO_4	$Lu_{0.162}Gd_{0.823}VO_4$	$Lu_{0.465}Gd_{0.52}VO_4$
P_{th} (W)	2.6	2.2	2.1	2.5	2.9
Host	$KLu(WO_4)_2$	$NaGd(WO_4)_2$	$YAl_3(BO_3)_4$	$GdCa_4O(BO_3)_3$	$Ca_3(NbGa)_{2-x}Ga_3O_{12}$
P_{th} (W)	0.51	0.58	0.62	0.51	0.48

*Experimental conditions: a plano-concave resonator formed by a plane high reflector and a T = 0.5%, 50-mm radius-of-curvature concave output coupler (cavity length ~50 mm). All crystals were of high optical quality, uncoated, 2-3 mm thick, with cross section of 3.3 × 3.3 mm^2; their small-signal absorption at the pump wavelength was 40–85%. Efficient laser operation was achieved with all of these crystals with slope efficiencies ranging from 50% to 80%.

We have observed bistable laser operation also in other Yb-doped vanadates including Yb:YVO_4, Yb:$GdVO_4$, and Yb:$Lu_xGd_{1-x}VO_4$. We studied several other different Yb-doped crystals, such as $KLu(WO_4)_2$, $NaGd(WO_4)_2$, $YAl_3(BO_3)_4$, $GdCa_4O(BO_3)_3$, $Ca_3(NbGa)_{2-x}Ga_3O_{12}$, etc., looking for bistable laser operation, but with none of them was it possible to observe a hysteresis loop in the input-output characteristics. Thus optical bistability seems to be a common feature only of the Yb-doped vanadate lasers. What distinguishes the Yb-doped vanadates studied by us from other Yb-doped crystals are the higher pump levels required to reach the laser threshold under identical resonator conditions (Table 1). As can be seen from the table, the laser thresholds of the Yb-doped vanadate lasers were roughly 3–5 times higher than those of the other crystals. The (resonant) losses responsible for the increased thresholds of the Yb-doped vanadate lasers might be strongly dependent on the crystal temperature and the same holds for the magnitude of the observed bistability effect.

6. CONCLUSION

In summary, high-power laser performance of both *a*-cut and *c*-cut Yb:$LuVO_4$ crystals was investigated by diode end pumping based on a simple plano-concave resonator. With an uncoated 2 mm *a*-cut crystal, a maximum output power of 8.3 W in π-polarization was generated with an optical-to-optical efficiency of 59%. The slope efficiency reached prior to the appearance of output roll-off was as high as 80%. We note that very recently, yet higher output powers (13 W) were achieved with Yb:$LuVO_4$ of the same doping level employing the thin disk laser geometry.[18]

Linearly polarized laser operation was obtained also with a *c*-cut crystal, for the first time to our knowledge with a vanadate laser, in which two orthogonal polarization components were present simultaneously with the electric vectors parallel to the [110] and $[\bar{1}10]$ crystallographic directions. The maximum output power attained in this case was 4.5 W, with an optical efficiency of 33% and a slope efficiency of 40%. We have also observed, for the first time to our knowledge, sizable optical bistability in the operation of the diode-pumped Yb:$LuVO_4$ laser, which is attributed to resonant absorption losses in the active medium affected by the thermal load. Significant output fluctuations occur in the transition region near the up-threshold, which is in agreement with theoretical predictions. Such optical bistability seems common to all Yb-doped vanadate lasers. The bistability in the case of Yb:$LuVO_4$ was confirmed also in other laser configurations.[18]

Finally, we measured the nonlinear index of refraction of Yb:$LuVO_4$, a parameter which is important for experiments aiming at higher peak powers like Q-switching and mode-locking or amplification with Yb:$LuVO_4$.

ACKNOWLEDGMENTS

This work was supported by the EU project DT-CRYS, NMP3-CT-2003-505580, the National Natural Science Foundation of China (No. 50572054), and the Excellent Young Teachers Program of MOE, China.

REFERENCES

[1] C. Maunier, J. L. Doualan, R. Moncorgé, A. Speghini, M. Bettinelli, and E. Cavalli, “Growth, spectroscopic characterization, and laser performance of Nd:$LuVO_4$, a new infrared laser material that is suitable for diode pumping,” J. Opt. Soc. Am. B **19**, 1794–1800, 2002.

[2] J. Liu, H. Zhang, Z. Wang, J. Wang, Z. Shao, M. Jiang, and H. Weber, „Continuous-wave and pulsed laser performance of Nd:$LuVO_4$ crystal,“ Opt. Lett. **29**, 168–170, 2004.

[3] X. Mateos, J. Liu, H. Zhang, J. Wang, M. Jiang, U. Griebner, and V. Petrov, „Continuous-wave and tunable laser operation of Tm:$LuVO_4$ near 1.9 µm under Ti:sapphire and diode laser pumping,” Phys. Stat. Sol. (a) **203**, R19-R21, 2006.

[4] C. Kränkel, D. Fagundes-Peters, S. T. Fredrich, J. Johannsen, M. Mond, G. Huber, M. Bernhagen, and R. Uecker, „Continuous wave laser operation of Yb^{3+}:YVO_4,“ Appl. Phys. B **79**, 543–546, 2004.

[5] V. E. Kisel, A. E. Troshin, N. A. Tolstik, V. G. Shcherbitsky, N. V. Kuleshov, V. N. Matrosov, T. A. Matrosova, and M. I. Kupchenko, “Spectroscopy and continuous-wave diode-pumped laser action of Yb^{3+}:YVO_4,” Opt. Lett. **29**, 2491-2493, 2004.

[6] J. Petit, B. Viana, P. Goldner, D. Vivien, P. Louiseau, and B. Ferrand, “Laser oscillation with low quantum defect in Yb:$GdVO_4$, a crystal with high thermal conductivity,” Opt. Lett. **29**, 833–835, 2004.

[7] J. Liu, X. Mateos, H. Zhang, J. Wang, M. Jiang, U. Griebner, and V. Petrov, „Continuous-wave laser operation of Yb:$LuVO_4$,“ Opt. Lett. **30**, 3162–3164, 2005.

[8] V. Peters, A. Bolz, K. Petermann, and G. Huber, “Growth of high-melting sesquioxides by the heat exchanger method,” J. Cryst. Growth **237–239**, 879–883, 2002.

[9] Y. Terada, K. Shimamura, V. V. Kochurikhin, L. V. Barashov, M. A. Ivanov, and T. Fukuda, “Growth and optical properties of $ErVO_4$ and $LuVO_4$ single crystals,” J. Cryst. Growth **167**, 369-372, 1996.

[10] M. Sheik-Bahae, A. A. Said, D. J. Hagan, M. J. Soileau, E. W. Van Stryland, “Nonlinear refraction and optical limiting in thick media,” Opt. Eng. **30**, 1228-1235, 1991.

[11] A. G. Selivanov, I. A. Denisov, N. V. Kuleshov, and K. V. Yumashev, “Nonlinear refractive properties of Yb^{3+}-doped $KY(WO_4)_2$ and YVO_4 laser crystals,” Appl. Phys. B **83**, 61-65, 2006.

[12] A. Owyoung and P. Esherick, “Stress-induced tuning of a diode-laser-excited monolithic Nd:YAG laser,” Opt. Lett. **12**, 999–1001, 1987.

[13] B. Zhou, T. J. Kane, G. J. Dixon, and R. L. Byer, "Efficient, frequency-stable laser-diode-pumped Nd:YAG laser," Opt. Lett. **10**, 62–64, 1985.

[14] S. Ruschin and S. H. Bauer, „Bistability, hysteresis and critical behavior of a CO_2 laser, with SF_6 intracavity as a saturable absorber," Chem. Phys. Lett. **66**, 100–103, 1979.

[15] J. M. Oh and D. Lee, "Strong optical bistability in a simple L-band tunable erbium-doped fiber ring laser," IEEE J. Quantum Electron. **40**, 374–377, 2004.

[16] T. G. Dziura, "Beyond mean field and plane wave theories of bistable semiconductor lasers," IEEE J. Quantum Electron. **22**, 651–654, 1986.

[17] L. A. Lugiato, P. Mandel, S. T. Dembinski, and A. Kossakowski, "Semiclassical and quantum theories of bistability in lasers containing saturable absorbers," Phys. Rev. A **18**, 238–254, 1978.

[18] C. Kränkel, R. Peters, K. Petermann, and G. Huber, „High power operation of $Yb:LuVO_4$ and $Yb:YVO_4$ crystals in the thin-disk laser setup", Advanced Solid-State Photonics, Jan. 28-31, 2007 (Vancouver, Canada), Online Conference Program.